ELSEVIER

European Journal of Cancer 41 (2005) 1453–1459

European Journal of Cancer

www.ejconline.com

Choline and phosphatidylcholine fluorescent derivatives localization in carcinoma cells studied by laser scanning confocal fluorescence microscopy

Anna M. Villa [a,b,1], Elvira Caporizzo [c,1], Antonio Papagni [b,d], Luciano Miozzo [b,d], Paola Del Buttero [e], Maria Donata Grilli [e], Nadia Amboldi [f], Ferruccio Fazio [c], Silvia M. Doglia [a,b], Barbara Giglioni [c,*]

[a] *Department of Biotechnologies and Biosciences, University of Milano-Bicocca, P.zza della Scienza 2, 20126 Milan, Italy*
[b] *INFM, UdR Milano-Bicocca, Via Roberto Cozzi 53, 20126 Milan, Italy*
[c] *IBFM-CNR, University of Milano-Bicocca, Scientific Institute H San Raffaele,Via Fratelli Cervi 93, 20090 Segrate, Milan, Italy*
[d] *Department of Material Sciences, University of Milano-Bicocca, Via Roberto Cozzi 53, 20126 Milan, Italy*
[e] *Department of Organic and Industrial Chemistry, University of Milano, Via Golgi 19, 20133 Milan, Italy*
[f] *Nerviano Medical Science srl, Viale Pasteur 10, 20014 Nerviano, Milan, Italy*

Received 21 October 2004; received in revised form 27 January 2005; accepted 2 February 2005
Available online 23 May 2005

Abstract

In this study, we have shown the intracellular distribution of choline and phosphatidylcholine fluorescent derivatives in human breast carcinoma cells using confocal microscopy. The fluorescent choline derivatives ethanamimium 2-hydroxy-*N*,*N*-dimethyl-*N*-[2-*N*-(2,1,3-benzoxadiazol-4-amine,-*N*-methyl,-7- nitro)-ethyl] bromide (NBD-choline) and C_6–NBD–phosphatidylcholine (C_6–NBD–PC) were used in this work. NBD-choline was easily internalised into drug sensitive MCF-7 and in multidrug resistant MCF-7/DX cells. The probe was found to localise in the endoplasmic reticulum of sensitive cells and in the Golgi of multidrug resistant cells. In contrast, very low accumulation was found in normal MCF10A cells. For C_6–NBD–PC, a similar pattern of localisation was found in tumour cells, but a significant uptake was also observed in normal cells. Unlike NBD-choline, C_6–NBD–PC appears not to discriminate between normal and tumour cells. These results are consistent with previously published results showing higher levels of ^{11}C-choline uptake in malignant lesions seen with positron emission tomography (PET) *in vivo* imaging. Our results suggest that using NBD-choline and laser scanning confocal fluorescence microscopy (LSCFM) could be a useful tool to study choline metabolism in cancer cells and to consolidate PET imaging findings.

Keywords: Choline fluorescent derivative; C_6–NBD–phosphatidylcholine; Laser scanning confocal fluorescence microscopy; Breast carcinoma cells; Choline metabolism; Positron emission tomography

1. Introduction

Neoplastic transformation is a multi-step phenomenon triggered by genetic and environmental hits resulting in alterations in the cell cycle, apoptosis, cell differentiation and metabolism. An altered phospholipid metabolism, whose hallmarks are enhanced choline uptake and increased phosphorylcholine and choline metabolite levels, has been found in a variety of cancers [1,2] and cancer cell lines [3–5].

The elevated choline transport and phosphorylation of cancer cells have been used for *in vivo* imaging by

* Corresponding author. Tel.: +39 0221717504; fax: +39 0221717558.
E-mail address: barbara.giglioni@ibfm.cnr.it (B. Giglioni).
[1] A.M.V. and E.C. contributed equally to this work.

0959-8049/$ - see front matter © 2005 Elsevier Ltd. All rights reserved.
doi:10.1016/j.ejca.2005.02.028

positron emission tomography (PET) of several malignant lesions. PET has proven to be a valuable non-invasive technique that allows the detection of different malignant tumours by means of suitable radiotracers such as [^{11}C]-choline [6–9]. However, [^{11}C]-choline PET shows limited sensitivity in discriminating between malignant neoplasia and other pathologies with enhanced choline metabolism such as inflammatory tissue [10,11]. The study of choline metabolism in cancer cells and its involvement in cell growth and transformation will be potentially useful in identifying tumour alterations that could be exploited in PET detection of malignant lesions.

Choline metabolism occurs through a cascade of three enzymes in the Kennedy pathway resulting in the biosynthesis of phosphatidylcholine. The control of subcellular distribution of compartments involved in choline metabolism has been shown to be implicated in the regulation of metabolism itself [12]. The enzymes that regulate the biosynthesis and hydrolysis of phosphatidylcholine have been extensively studied and their subcellular localisation defined [13–17]. However, in living cancer cells, little is known about the localisation of choline, its metabolites and the cell compartments involved in phospholipid metabolism. The study of the intracellular localisation of choline in cancers by means of suitable fluorescent probes is of great interest and is hoped to ultimately characterise choline metabolism in tumours. The aim of this study was to identify in living cells and at the single-cell level, the subcellular compartments and organelles that are involved in choline metabolism in tumour cell lines. To this end, we undertook a confocal fluorescence microscopy study to define the intracellular localisation of choline using a newly synthesized fluorescent choline probe.

2. Materials and methods

2.1. C_6–NBD–phosphatidylcholine and NBD-choline synthesis

The synthesis of ethanamimium,2-hydroxy-*N*,*N*-dimethyl-*N*-[2-*N*-(2,1,3-benzoxadiazol-4-amine,-*N*-methyl,-7-nitro)-ethyl] bromide (NBD-choline) has been described in detail in Appendix A and Fig. A.1. C_6–NBD–phosphatidylcholine (C_6–NBD–PC) was purchased from Molecular Probes, Eugene, USA).

2.2. Cell culture

The parental drug-sensitive human breast carcinoma MCF-7 cell line and its derivative MDR variant (MCF-7/DX) were cultured as a monolayer in RPMI 1640 medium (EuroClone Ltd., UK) supplemented with 10% v/v Fetal Calf Serum (FCS), 100 units/ml penicillin, 0.1 mg/ml streptomycin and 2 mM L-glutamine at 37 °C in a humidified 5% CO_2 atmosphere. The immortalised epithelial cell line MCF10A was grown in DMEM medium (Gibco, Invitrogen) supplemented with 10% v/v FCS, 10 μg/ml Insulin, 0.5 μg/ml Hydrocortisol and 20 ng/ml EGF at 37 °C in a 5% CO_2 humidified atmosphere. MCF-7, MCF-7/DX and MCF10A cells were kindly provided by Nerviano Medical Science, Milan.

Prior to experimentation, P-glycoprotein (P-gp) expression in MCF-7, MCF-7/DX and MCF10A was measured by RT-PCR with specific oligonucleotide pairs. A high level of P-gp transcript was found in the multidrug resistant MCF-7/DX while P-gp expression was not found in MCF-7 and MCF10A.

For the confocal fluorescence microscopy, cells were grown in the appropriate medium in Petri dishes, incubated for 2 min in the presence of NBD-choline (50 μM), or for 15 min in the presence of C_6–NBD–PC (5 μM). Cells were then washed with PBS and incubated in RPMI medium for 0, 15, 40 and 75 min. Confocal microscopy observations were made immediately (time 0) and after 15, 40 and 75 min.

2.3. Toxicity of NBD-choline

Cell viability was tested with the CellTiter-Glo™ Luminescent Cell Viability Assay (Promega), which allowed an evaluation of cellular ATP levels. Cellular ATP levels are thought to be proportional to the number of metabolically active viable cells. The assay procedure required the addition of cell lysis buffer, the enzyme firefly luciferase and its substrate luciferin to the cells. In the presence of cellular ATP released after lysis, the luciferase enzyme converted the luciferin to oxyluciferin in a light-producing reaction. The amount of light given out was recorded by a luminometer, was proportional to the amount of ATP and directly correlated to the number of viable cells. Using this assay, we tested the toxicity of the newly synthesized NBD-choline on MCF-7, MCF-7/DX and MCF10A cell lines that were incubated with the labeled choline at different concentrations (200, 100, 50, 25 and 12.5 μM) for 15, 40 and 75 min. The cells were then washed, incubated in RPMI medium for 72 h and tested for cell viability.

In addition, we tested the effect of NBD-choline on cell proliferation by measuring 5-bromo-2′-deoxyuridine (BrdU) incorporation into newly synthesized DNA using the light immunoassay DELFIA Cell Proliferation Kit (Perkin–Elmer). The evaluation of the amount of incorporated BrdU (and consequently the number of viable cells) was performed after 15 min of incubation with NBD-choline, overnight BrdU labelling and 24 h of recovery in RPMI medium alone. Incorporated BrdU was detected using a europium labeled mouse monoclonal antibody 1:100 (stock solution 50 μg/ml) according to the manufacturer instructions. To allow antibody

detection, the cells were fixed by denaturing DNA using a Fix Solution containing ethanol. Unbound antibody was washed away, and DELFIA Inducer was added to dissociate the europium ions from the labeled antibody to form highly fluorescent chelate-complexes with components of the DELFIA Inducer. The fluorescence measured by a luminometer was proportional to the DNA synthesised in the cell population.

2.4. Laser scanning confocal fluorescence microscopy

The images of NBD-choline and C_6–NBD–PC fluorescence in living cells were obtained using a laser scanning confocal microscope MRC-600 Bio-Rad (Hemel Hempstead, UK) coupled with an epifluorescence microscope Nikon Optiphot-2. An oil immersion objective Nikon Planapochromat 60× (N.A. 1.4) was also employed. The dye fluorescence excitation was carried out by 25 mW Ar ion laser at 488 nm, a wavelength falling within the absorption band of NBD-moiety. Both NBD-choline and C_6–NBD–PC fluorescence were observed through a long pass filter, transmitting wavelengths longer than 515 nm. A photon counting system was employed to detect the fluorescence signal. This sensitive detection allowed the reduction of the laser excitation power to 0.1 mW at the entry of the optical head, enabling us to preserve cell viability during measurements and to collect good fluorescence images of the two probes at low concentrations [18].

3. Results

In the present study, the intracellular distribution of choline and phosphatidylcholine was investigated using laser scanning confocal fluorescence microscopy (LSCFM) in breast carcinoma MCF-7 cells. These cells represent a good model system where choline metabolism alterations have been extensively characterised [4,5]. In addition, the multidrug resistant sub-line MCF-7/DX and the normal breast epithelial MCF10A cells were also examined. To investigate choline metabolism by LSCFM, a new fluorescent derivative of choline (NBD-choline) was synthesized and used in addition to the commercially available C_6–NBD–phosphatidylcholine (C_6–NBD–PC).

3.1. Synthesis of NBD-choline

To follow choline localisation in live normal and tumour cells through LSCFM fluorescence detection, a new fluorescent derivative, NBD-choline, was expressly synthesised by anchoring a fluorescent moeity to one of the three methyl groups on the nitrogen atom of the choline structure. Derivatisation at this site is not expected to interfere with the biological functions of the choline-hydroxyethyl chain. Details of synthesis can be found in Appendix B and Fig. A.1.

3.2. NBD-choline intracellular localisation

A good fluorescence signal from NBD-choline was observed by LSCFM in carcinoma cells (Fig. 1(a) and (b)) indicating that the newly synthesized probe had internalised well in these cells. In the immortalized MCF10A cells (Fig. 1(c)) a low signal, comparable to intrinsic background cell fluorescence, was found. These results are in agreement with the data obtained by PET analysis in several malignant neoplasia, where ^{11}C-choline uptake was found to be greater in tumour lesions than in the normal tissue [6–9]. Furthermore, as can be seen by the comparison of Fig. 1(a) and (b), the intracellular distribution of NBD-choline in drug-sensitive MCF-7 cells is different from that of multidrug resistant MCF-7/DX cells. In sensitive cells, NBD–choline fluorescence was localised to the endoplasmic reticulum (ER) (Fig. 1(a)). In additions intense spots were observed superimposed to the ER diffuse fluorescence. In contrast, multidrug resistant cells had a weak fluorescence signal in ER with intense signals localised to the Golgi apparatus. The Golgi pattern was very similar to that observed in the same cell line for NBD-ceramide [19], a well known vital fluorescent probe of the Golgi system [20–22]. The viability of cells treated with the NBD-choline probe was similar to control cells and no appreciable differences were found in cellular growth as quantified by ATP levels and BrdU incorporation (data not shown).

3.3. C_6–NBD–phosphatidylcholine intracellular localisation

It is already known [21,23] that the C_6–NBD–PC probe is a non toxic, easily internalised probe that gives stable fluorescent signal. The intracellular localisation of C_6–NBD–PC was investigated and compared to NBD-choline. A similar intracellular localisation was observed for both NBD-choline and C_6–NBD–PC in carcinoma cells. In sensitive MCF-7 cells, C_6–NBD–PC was found mainly in ER (Fig. 2(a)). In drug-resistant MCF-7/DX cells (Fig. 2(b)) the probe was localised in the Golgi apparatus and to a smaller extent to the ER with lower fluorescence intensity. The pattern of localisation was very similar to that of NBD-choline (Fig. 1). In immortalised MCF10A cells (Fig. 2(c)), a diffused C_6–NBD–PC fluorescence was observed throughout the cytoplasm. The nuclear and plasma membranes also gave fluorescence signal as was seen by line profile analysis (data not shown). The fluorescent patterns found in this study for NBD-choline and C_6–NBD–PC localisation are constant in time within a few hours after incubation.

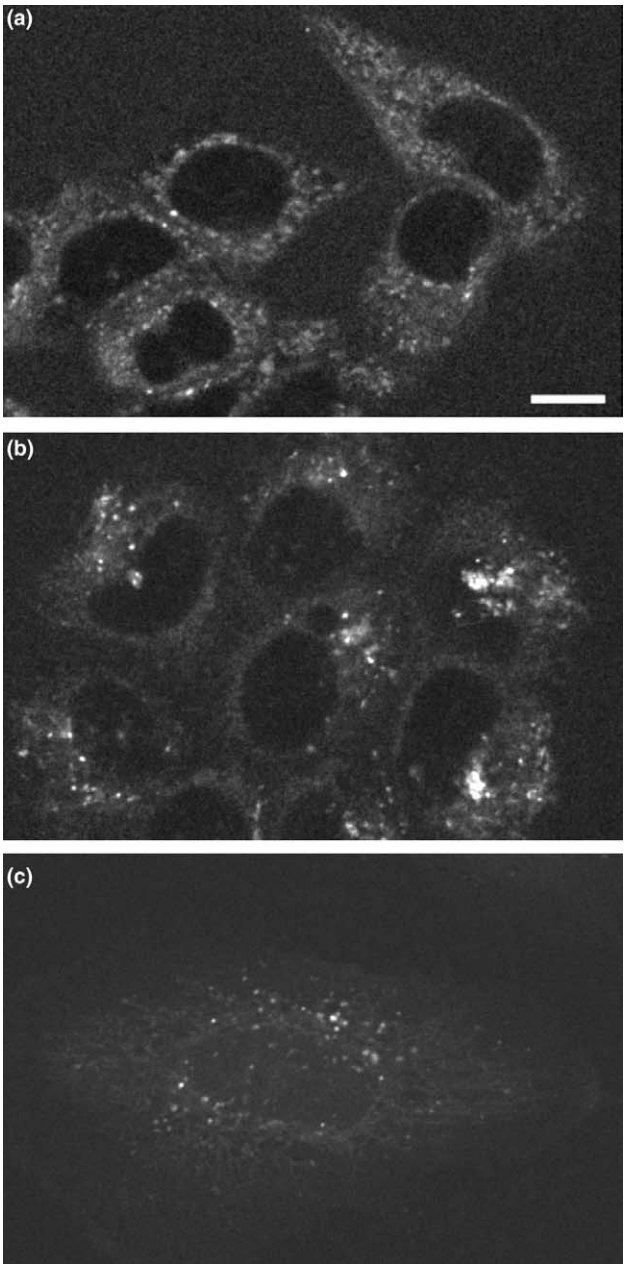

Fig. 1. LSCFM image of NBD-choline in carcinoma and normal breast epithelial cells. (a) sensitive carcinoma MCF-7 cells; (b) multidrug resistant carcinoma MCF-7/DX cells; (c) normal immortalized MCF10A cells. To allow the visual inspection of MCF10A cell fluorescence, the data in subpart c were intensified by a factor 3. Scale bar: 10 μm.

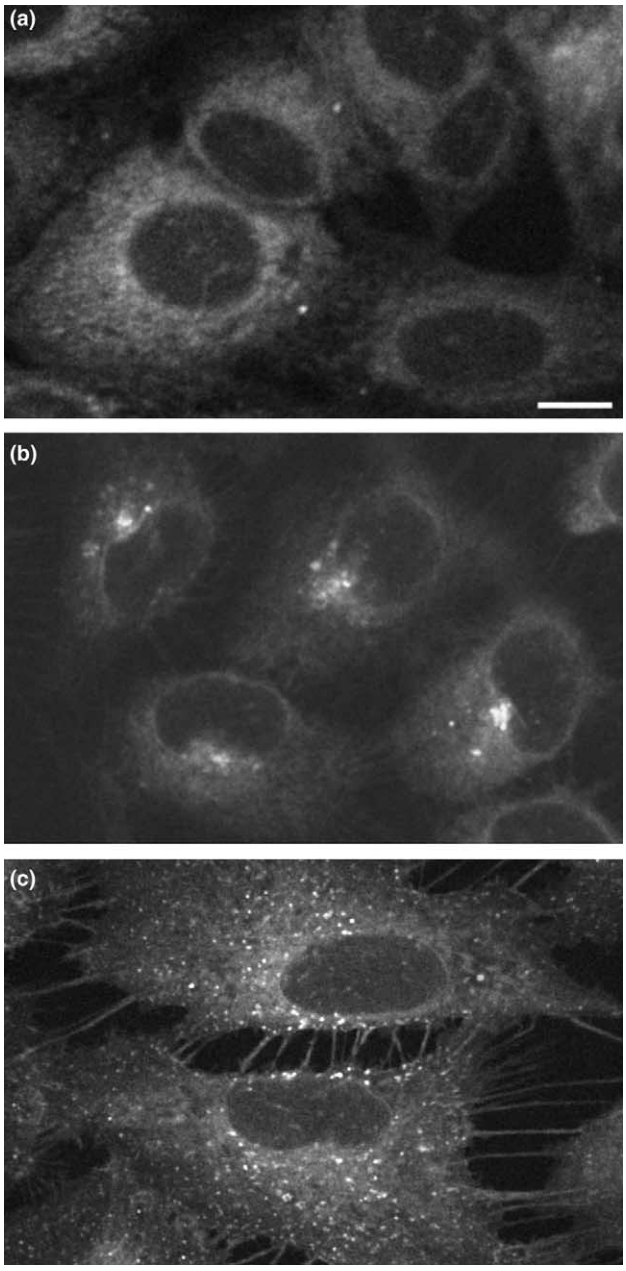

Fig. 2. LSCFM image of C_6–NBD–phosphatidylcholine in carcinoma and normal breast epithelial cells. (a) sensitive carcinoma MCF-7 cells; (b) multidrug resistant carcinoma MCF-7/DX cells; (c) normal immortalized MCF10A cells; Scale bar: 10 μm.

4. Discussion

The newly synthesised fluorescent NBD-choline, designed to probe choline uptake and distribution in living cells, has been successfully used in this LSCFM study to visualise the intracellular compartments involved in choline metabolism and choline-phospholipid biosynthesis in human breast tumour and normal cell lines. In particular, NBD-choline was found to predominantly localise in the ER of drug-sensitive MCF-7 cells and in the Golgi apparatus of multidrug resistant MCF-7/DX cells. This difference in NBD-choline distribution between drug-sensitive and drug resistant cell lines suggests for the first time that MDR cells have changed choline metabolic pathways. As it is well documented in a recent review by Vance and Vance [16], important steps of phospholipid biosynthesis pathway take place in the ER and mitochondrial membranes at contact regions with ER, known as mitochondria-associated membranes (MAM) [24]. The fluorescent spots observed in drug-sensitive

cells could be assigned to NBD-choline in these MAM regions. It should be noted that these structures are not seen in the drug resistant cell line, where ER displays a weaker fluorescence and NBD-choline accumulates in the Golgi.

Phosphatidylcholine shows an intracellular distribution in MCF-7 and in MCF-7/DX carcinoma cells similar to that of NBD-choline. C_6–NBD–PC localised to the ER of drug-sensitive cells and in the Golgi of MDR cells. Interestingly, it has been shown that P-glycoprotein, that is overexpressed in multidrug resistant MCF-7/DX cells, is also localised to the *trans*-Golgi vescicles [25]. Also, in drug resistant CEM/VBL300 cells, C_6–NBD–PC appears to be a substrate of P-gp [26]. All these results suggest that NBD-choline and C_6–NBD–PC in MDR MCF-7/DX cells may be substrates of P-gp that is responsible for cell detoxification and cell membrane phospholipid traffic leading to lower intracellular accumulation of the two probes. Moreover, intracellular lipid transport is fundamental for the dynamics of subcellular membrane architecture and defining a given membrane environment could regulate the multidrug resistance activity of P-gp itself [27].

We have also shown that NBD-choline enters almost exclusively into cancer cells and not in normal cells, a result that confirms *in vivo* imaging by ^{11}C-choline-PET of several human tumours. Opposite to what was found for NBD-choline (Fig. 1(c)), C_6–NBD–PC entered efficiently into MCF10A cells (Fig. 2(a)). While C_6–NBD–PC entered both normal and cancer cells, NBD-choline is actively transported and accumulated only in malignant cells in which choline metabolism and uptake are enhanced [4,5].

In this context, NBD-choline could be considered a new valuable fluorescent probe for detecting and characterising malignant cells with deregulated choline metabolism and for studying the first steps of its metabolism in transformed cells. It is also possible to speculate that LSCFM could be combined with *in vivo* PET studies to provide a better cancer detection and provide valuable support to PET oncological applications. In addition, the results of this study have shown the specificity of choline uptake by cancer cells and highlight the possibility of designing new choline derivatives that can be specifically targeted to tumour cells for anticancer activity.

Conflict of interest statement

None declared.

Appendix A

All reagents, solvents and starting materials, 4-chloro, 7-nitro, 2,1,3-benzoxadiazole (NBD-Cl); *N*-methylethanolamine,*N*,*N*-dimethylethanolanime, methylethylketone, methylene chloride, triphenylphosphine and *N*-bromo-succinimide, were purchased from commercial suppliers (Aldrich, Fluka) and used without further purification. Thin layer chromatographic analyses (tlc) were performed on silica gel-G (Merck) coated plates, and column chromatography purification was performed using silica gel (230–400 mesh) from Merck. The synthesis of 2-[methyl(7-nitro-2,1,3-benzoxadiazol-4-yl)amino]-ethanol 2 (see Fig. A.1) was done as described in the literature [28].

Synthesis of 1-bromo,2-[methyl(7-nitro-2,1,3-benzoxadiazol-4-yl)amino]-ethane 3 (Fig. A.1): compound **2** (0.2 g, 0.84 mmol) was dissolved in dry CH_2Cl_2 (10 ml); Ph_3 P (0.44 g, 1.68 mmol) was added and the solution was cooled to 0 °C, and NBS (0.4 g, 1.68 mmol) was added portion wise over 5 min under continuous stirring. The solution was stirred at 0 °C following the reaction by thin layer chromatography (tlc) (eluent CH_2Cl_2/AcOEt, 7:3). After 1.5 h the reaction was practically concluded; the solvent was then evaporated under reduced pressure and the crude reaction mixture was purified by column chromatography over silica gel (eluent CH_2Cl_2/AcOEt, 7:3), affording 0.201 g of analytically pure **3** (79% yield).

Data for **3**: orange solid, m.p. 122–123 °C; ^{1}H NMR ($CDCl_3$, 300 MHz), ppm: 3.53 (s, 3H, N–CH_3), 3.70 (t, 2H, J = 6.6 Hz, CH_2 Br), 4.58 (t, 2H, J = 6.6 Hz, CH_2–NMe), 6.21 (d, 1H, J = 8.9 Hz, furazane nucleus), 8.49 (d, 1H, J = 8.9 Hz, furazane nucleus); Elemental Anal. Calcd for $C_9H_9BrN_4O_3$: C, 35.90; H, 3.01; N, 18.61. Found: C, 35.12; H, 2.89; N, 17.98.

Synthesis of the ethanamimium,2-hydroxy-*N*,*N*-dimethyl-*N*-[2-*N*-(2,1,3-benzoxadiazol-4-amine,-*N*-methyl,-7-nitro)-ethyl] bromide **1** (Figs. 1 and A.1). A solution of compound **3** (0.2 g, 0.66 mmol) in dry methylethylketone (15 ml) was refluxed for 48 h with the *N*,*N*-dimethylethanolamine (2 ml). The formed precipitate was filtered off and washed several times with dry acetone, giving 0.103 g analytically pure **1** (40% yield).

Data for **1**: orange solid, IR: 3250 cm^{-1} (νOH, broad band); ^{1}H NMR ($CDCl_3$ + DMSO, 300 MHz), ppm: 3.47 (s, 3H, N–CH_3), 3.59 (m, 2H, CH_2–OH), 3.79 (t, 2H, J = 6.6 Hz, CH_2 Br), 3.93 (m, 8H, CH_2 + 2 CH_3) 4.60 (t, 2H, J = 6.6 Hz, CH_2–NMe), 5.36 (broad s, 1H, OH), 6.44 (d, 1H, J = 9.0 Hz, furazane nucleus), 8.48 (d, 1H, J = 9.0 Hz, furazane nucleus); MALDI-TOF:

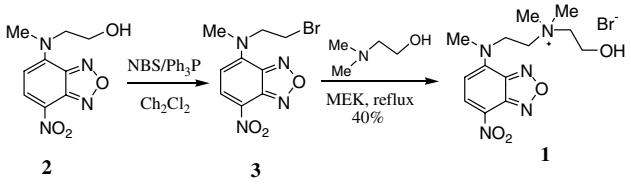

Fig. A.1. Synthesis of the NBD-choline derivative 1.

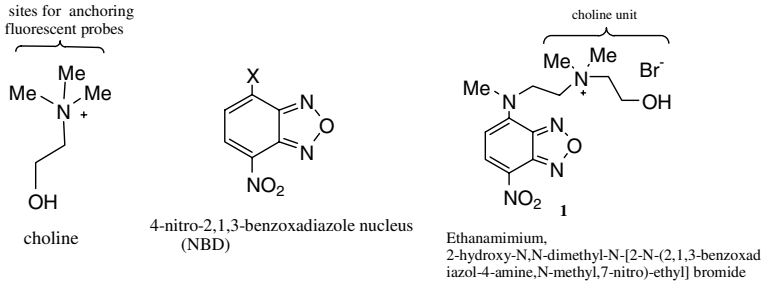

Fig. A.2. Molecular structure of the NBD-choline derivative 1.

310 ($M^+ - Br$). Elemental Anal. Calcd for C_{13} H_{20} BrN_5O_4: C, 40.01; H, 5.17; N, 17.95. Found: C, 38.85; H, 4.89; N, 17.32%.

Appendix B

Our choice of the 4-nitro-2,1,3-benzoxadiazole nucleus (NBD) as the fluorescent probe was due to its being commonly exploited in many biological system studies. It was also planned that this unit would be anchored to the choline moiety by an aminoethyl chain as in the ethanaminium,2-hydroxy-*N*,*N*-dimethyl-*N*-[2-*N*-(2,1,3-benzoxadiazol-4-amine,-*N*-methyl,-7-nitro)-ethyl] bromide (see Fig. A.2 for the molecular formula) since this solution guarantees high NBD nucleus fluorescence. The synthesis of ethanaminium,2-hydroxy-*N*,*N*-dimethyl-*N*-[2-*N*-(2,1,3-benzoxadiazol-4-amine,*N*-methyl, 7-nitro)-ethyl] bromide (compound 1, NBD-choline), was carried out starting from *N*-methyl,*N*-(2hydroxy)-ethyl-4-amino, 7-nitro, 2,1,3-benzoxadiazole (compound 2), prepared as described in the literature [28], which was then transformed into the bromoethyl derivative (compound 3) by means of an OH/bromine exchange carried out with *N*-bromosuccinimide (NBS) in the presence of triphenylphosphine [29]. Finally, compound 3 was reacted in boiling methylethylketone (MEK) with *N*,*N*-dimethyl-ethanolamine to afford the expected salt compound **1** in satisfactory yields [30] (Fig. A.1).

The optical absorption and fluorescence of NBD-choline are similar to those reported in the literature for NBD-amino derivatives[31–33], displaying maxima at 479 and 541 nm, respectively.

References

1. Roebuck J, Cecil K, Schnall M, *et al*. Human breast lesions: characterization with proton MR spectroscopy. *Radiology* 1998, **209**, 269–275.
2. Podo F. Tumour phospholipid metabolism. *NMR Biomed* 1999, **12**, 413–439.
3. Katz-Brull R, Margalit R, Bendel P, *et al*. Choline metabolism in breast cancer; ^{2}H-, ^{13}C- and ^{31}P-NMR studies of cells and tumors. *Magma* 1998, **6**, 44–52.
4. Aboagye EO, Bhujwalla ZM. Malignant transformation alters membrane choline phospholipid metabolism of human mammary epithelial cells. *Cancer Res* 1999, **59**, 80–84.
5. Katz-Brull R, Seger D, Rivenson-Segal D, *et al*. Metabolic markers of breast cancer: enhanced choline metabolism and reduced choline–ether–phospholipid synthesis. *Cancer Res* 2002, **62**, 1966–1970.
6. Hara T, Kosaka N, Kishi H. PET imaging of prostate cancer using carbon-11-choline. *J Nucl Med* 1998, **39**, 990–995.
7. DeGrado TR, Coleman RE, Wang S, *et al*. Synthesis and evaluation of 18F-labeled choline as an oncologic tracer for positron emission tomography: initial findings in prostate cancer. *Cancer Res* 2000, **61**, 110–117.
8. Hara T. 11C-choline and 2-deoxy-2-[18F]fluoro-D-glucose in tumor imaging with positron emission tomography. *Mol Imaging Biol* 2002, **4**, 267–273.
9. Picchio M, Messa C, Landoni C, *et al*. Value of [11C]choline-positron emission tomography for re-staging prostate cancer: a comparison with [18F]fluorodeoxyglucose-positron emission tomography. *J Urol* 2003, **169**, 1337–1340.
10. Roivainen A, Parkkola R, Yli-Kerttula T, *et al*. Use of positron emission tomography with methyl-11C-choline and 2-18F-fluoro-2-deoxy-D-glucose in comparison with magnetic resonance imaging for the assessment of inflammatory proliferation of synovium. *Arthritis Rheum* 2003, **48**, 3077–3084.
11. Wyss MT, Weber B, Honer M, *et al*. 18F-choline in experimental soft tissue infection assessed with autoradiography and high-resolution PET. *Eur J Nucl Med Mol Imaging* 2004, **31**, 312–316.
12. Tronchere H, Record M, Terce F, *et al*. Phosphatidylcholine cycle and regulation of phosphatidylcholine biosynthesis by enzyme translocation. *Biochim Biophys Acta* 1994, **1212**, 137–151.
13. Vance DE. Boehringer Mannheim Award lecture. Phosphatidylcholine metabolism: masochistic enzymology, metabolic regulation, and lipoprotein assembly. *Biochem Cell Biol* 1990, **68**, 1151–1165.
14. Higgins JA, Fieldsend JK. Phosphatidylcholine synthesis for incorporation into membranes or for secretion as plasma lipoproteins by Golgi membranes of rat liver. *J Lipid Res* 1987, **28**, 268–278.
15. Henneberry AL, Wright MM, McMaster CR. The major sites of cellular phospholipid synthesis and molecular determinants of fatty acid and lipid head group specificity. *Mol Biol Cell* 2002, **13**, 3148–3161.
16. Vance JE, Vance DE. Phospholipid biosynthesis in mammalian cells. *Biochem Cell Biol* 2004, **82**, 113–128.
17. Freyberg Z, Siddhanta A, Shields D. "Slip, sliding away": phospholipase D and the Golgi apparatus. *Trends Cell Biol* 2003, **13**, 540–546.
18. Doglia S, Bianchi L, Colombo R, *et al.* Laser scanning confocal fluorescence microscopy of living cells. In Korppi J, Tommola S, eds. *Laser applications in life science*. 1993, 126–134.

19. Villa AM, Doglia SM. Mitochondria in tumor cells studied by laser scanning confocal microscopy. *J Biomed Opt* 2004, **9**, 385–394.
20. Lipsky NG, Pagano RE. Sphingolipid metabolism in cultured fibroblasts: microscopic and biochemical studies employing a fluorescent ceramide analogue. *Proc Natl Acad Sci USA* 1983, **80**, 2608–2612.
21. Sleight RG, Pagano RE. Transport of a fluorescent phosphatidylcholine analog from the plasma membrane to the Golgi apparatus. *J Cell Biol* 1984, **99**, 742–751.
22. Calcabrini A, Villa AM, Molinari A, *et al*. Influence of N-methylformamide on the intracellular transport of doxorubicin. *Eur J Cell Biol* 1997, **72**, 61–69.
23. Struck D, Pagano R. Insertion of fluorescent phospholipids into the plasma membrane of a mammalian cell. *J Biol Chem* 1980, **255**, 5404–5410.
24. Stone SJ, Vance JE. Phosphatidylserine synthase-1 and -2 are localized to mitochondria-associated membranes. *J Biol Chem* 2000, **275**, 34534–34540.
25. Molinari A, Cianfriglia M, Meschini S, *et al*. P-glycoprotein expression in the Golgi apparatus of multidrug-resistant cells. *Int J Cancer* 1994, **59**, 789–795.
26. Bosch I, Dunussi-Joannopoulos K, Wu RL, *et al*. Phosphatidylcholine and phosphatidylethanolamine behave as substrates of the human MDR1 P-glycoprotein. *Biochemistry* 1997, **36**, 5685–5694.
27. Ferte J. Analysis of the tangled relationships between P-glycoprotein-mediated multidrug resistance and the lipid phase of the cell membrane. *Eur J Biochem* 2000, **267**, 277–294.
28. Kalinina O, Kumacheva E. A "Core-Shell" approach to producing 3D polymer nanocomposites. *Macromolecules* 1999, **32**, 4122–4129.
29. Williams M, Rapoport H. Synthesis of enantiomerically pure diethylenetriaminepentaacetic acid analogs. L-Phenylalanine as the educt for substitution at the central acetic acid. *J Org Chem*, 1151–1158.
30. Ghosh YK, Visweswariah SS, Bhattacharya S. Advantage of the ether linkage between the positive charge and the cholesteryl skeleton in cholesterol-based amphiphiles as vectors for gene delivery. *Bioconjug Chem* 2002, **13**, 378–384.
31. Heberer H, Matsciner H. UV, visible, and IR spectroscopic studies with *N*-substituted 4-amino-7-nitrobenzofurazans. *J Prakt Chem* 1986, **328**, 2261–2274.
32. Uchiyama S, Santa T, Fukushima T, *et al*. Effects of the substituent groups at the 4- and 7-positions on the fluorescence characteristics of benzofurazan compounds. *J Chem Soc: Perking Trans* 1998, **2**, 2165–2173.
33. Uchiyama S, Santa T, Imai K. Study on the fluorescent 'on-off' properties of benzofurazan compounds bearing an aromatic substituent group and design of fluorescent 'on-off' derivatization reagents. *Analyst* 2000, **125**, 1839–1845.